

Article

Atmospheric Dispersion of Radioactivity from Nuclear Power Plant Accidents: Global Assessment and Case Study for the Eastern Mediterranean and Middle East

Theodoros Christoudias ^{1,*}, Yiannis Proestos ¹ and Jos Lelieveld ^{1,2}

¹ The Cyprus Institute, 20 Konstantinou Kavafi Street, Aglantzia, Nicosia 2121, Cyprus; E-Mails: y.proestos@cyi.ac.cy (Y.P.); jos.lelieveld@mpic.de (J.L.)

² Max Planck Institute of Chemistry, Hahn-Meitner-Weg 1, Mainz 55128, Germany

* Author to whom correspondence should be addressed; E-Mail: christoudias@cyi.ac.cy; Tel.: +357-22-208-677; Fax: +357-22-208-625.

External Editor: Erich Schneider

Received: 24 October 2014; in revised form: 4 December 2014 / Accepted: 5 December 2014 /

Published: 12 December 2014

Abstract: We estimate the contamination risks from the atmospheric dispersion of radionuclides released by severe nuclear power plant accidents using the ECHAM/Modular Earth Submodel System (MESSy) atmospheric chemistry (EMAC) atmospheric chemistry-general circulation model at high resolution (50 km). We present an overview of global risks and also a case study of nuclear power plants that are currently under construction, planned and proposed in the Eastern Mediterranean and Middle East, a region prone to earthquakes. We implemented continuous emissions from each location, making the simplifying assumption that all potential accidents release the same amount of radioactivity. We simulated atmospheric transport and decay, focusing on ¹³⁷Cs and ¹³¹I as proxies for particulate and gaseous radionuclides, respectively. We present risk maps for potential surface layer concentrations, deposition and doses to humans from the inhalation exposure of ¹³¹I. The estimated risks exhibit seasonal variability, with the highest surface level concentrations of gaseous radionuclides in the Northern Hemisphere during winter.

Keywords: nuclear power plant accidents; radioactivity transport modeling; deposition and inhalation risks

1. Introduction

The International Atomic Energy Agency (IAEA) defines a nuclear accident as an event that releases radioactivity with significant consequences on a nuclear facility and the environment, including harmful doses to humans and soil contamination. Nuclear power plant accidents can have significant impacts on society and the environment, fueling the debate on the security of facilities and materials, planning and sustainability. Risk assessment for radioactivity contamination is necessary for mitigation strategy formulation and potential impact precautions by stakeholders, the development of policies by decision makers and public information at global, regional and national levels.

The radiological significance of nuclear events is categorized by the IAEA on the International Nuclear Event Scale (INES) with a numerical rating from one to seven. The INES categorization takes into account the impact on people and the environment and the degree of contamination by the emitted radioactivity. There have been two major accidents categorized at the most severe level of INES 7 that occurred in Chernobyl, Ukraine and the meltdown of three reactors at Fukushima, Japan, and a total of more than 20 accidents at the level of INES 4 or higher, categorized as accidents with at least local consequences.

Following previous studies [1–3], we have included all nuclear power plants worldwide that are currently operational (OP), under construction (UC) and planned or proposed (PL), based on the nuclear power plant (NPP) database compiled and published by the World Nuclear Association (WNA) [4]. In our simulations, we implemented constant continuous emissions from each NPP location and computed atmospheric transport and removal over a period of 20 years to warrant climatological representativeness. We used boundary conditions prescribed by a future intermediate climate change scenario in order to produce global overall and seasonal risk maps for near-surface concentrations and ground deposition of radioactivity from hypothetical nuclear power plant accidents. Furthermore, we estimated worldwide potential human doses from the inhalation of gaseous radioactivity and the exposure to deposited radionuclides transported in aerosol particles. The risk posed from nuclear power plant accidents is not limited to the national or even regional level, but can assume global dimensions. Many nations may be subjected to great exposure after severe accidents, even ones that are not pursuing nuclear energy as a means of power production [4].

The present paper both extends and complements the work of these previous studies by using higher resolution modeling and focusing on a test case in a particular region of interest, the Eastern Mediterranean and Middle East (EMME), where earthquakes are recurrent, being a risk factor for nuclear facilities. No assumption is made on the type, capacity or reactor core count to assess the probability of an accident happening at each particular location or the total emission magnitude. By employing unit emission sources, we assess the comparative potential risk and provide a scale for the absolute magnitude of any accident. It should be noted that we aim to capture the risk patterns related to the ensemble of meteorological conditions over the 20-year simulation rather than individual events, *i.e.*, taking a probabilistic approach. If an event were to happen, the absolute risks can be calculated by scaling our unit emissions by the real release of radioactivity, and by also accounting for the actual meteorological conditions during the accident, the concentrations and exposure can be calculated following a deterministic approach.

2. Methodology

The ECHAM/Modular Earth Submodel System (MESSy) atmospheric chemistry (EMAC) model is a numerical chemistry and climate simulation system that includes sub-models describing tropospheric and middle-atmosphere processes and their interaction with oceans, land and human influences [5]. It uses the second version of the Modular Earth Submodel System (MESSy2) to link multi-institutional computer codes. The core atmospheric general circulation model is the fifth generation European Centre Hamburg general circulation model, ECHAM5 [6].

For the present study, we applied EMAC (ECHAM5 version 5.3.02, MESSy version 2.42p2) at the T106L31 resolution, that is, with a spherical truncation of T106 (corresponding to a quadratic Gaussian grid of approximately 1.1 by 1.1 degrees in latitude and longitude, ~ 110 km at the equator) and at the T255L31 resolution, *i.e.*, with a spherical spectral truncation of T255 (corresponding to a quadratic Gaussian grid of approximately 0.5 by 0.5 degrees in latitude and longitude, ~ 50 km at the equator), with 31 vertical hybrid pressure levels up to 10 hPa [7].

The surface (skin) temperatures and sea ice distribution for the AMIP II simulations [8] between the years 2003 and 2009 were used as boundary conditions for the higher resolution run (7-year simulation) and from the IPCC [9] SRESA2 emissions scenario for the period 2010–2030 for the lower resolution run (20-year simulation). The applied model setup comprises the submodels, RAD4ALL for radiation and atmospheric heating processes, CLOUD for cloud formation and microphysical processes including precipitation and CONVECT for the vertical transport of trace species associated with shallow, mid-level and deep convection. The DRYDEP (dry deposition) [10] and SCAV (scavenging) [11,12] submodels were used to simulate aerosol dry and wet deposition processes, respectively. The SEDI (sedimentation) submodel was used to simulate particle sedimentation, of which the results will be presented below as part of the simulated dry deposition. The TREXP (tracer release experiments from point sources) submodel [5] was used to define tracers and emission sources.

The EMAC model uses a hybrid system for specifying atmospheric vertical levels. The system combines the constant pressure level system with the sigma level system based on surface pressure, such that closer to the surface of the Earth, the levels more closely resemble a pure sigma level, while higher up, the levels are close to constant pressure surfaces [13].

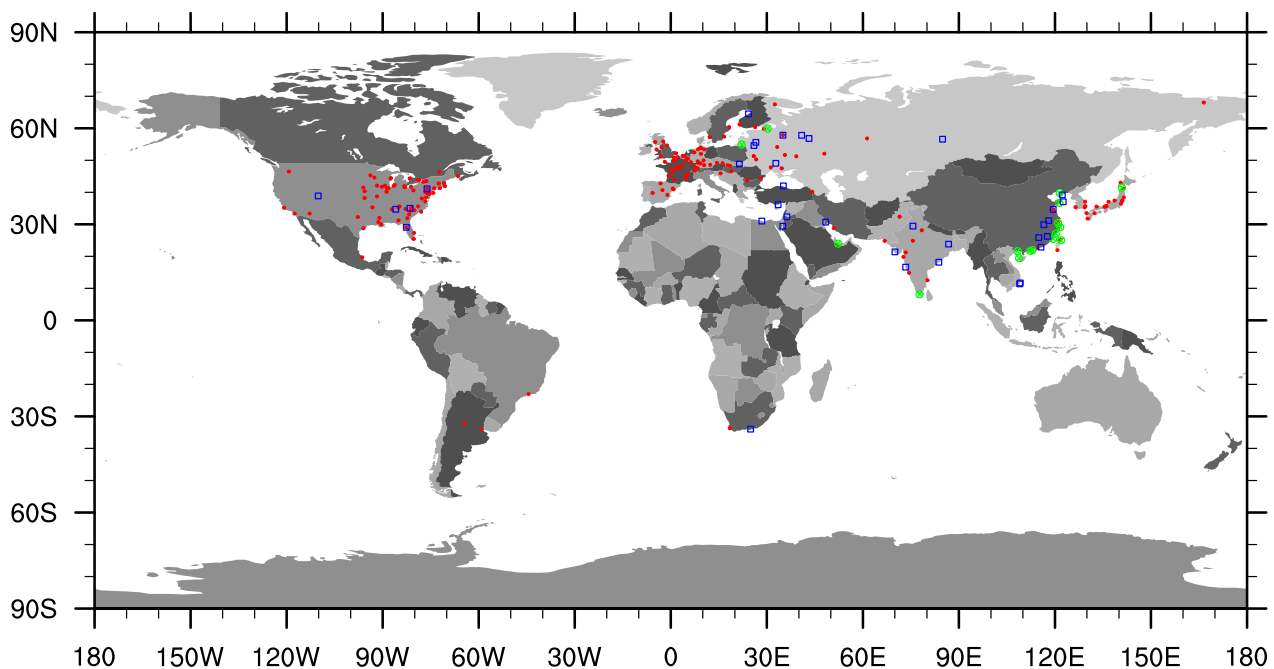
The model setup was evaluated using a real test case using emission estimates from the accident that occurred at the Fukushima Dai-ichi NPP. Radionuclide surface layer concentrations were compared with station measurements taken by a global monitoring network of the Comprehensive Nuclear Test Ban Treaty Organization (CTBTO) [14]. The modeling skill was evaluated using the radionuclide ^{133}Xe , a noble gas that behaves as a passive tracer, showing very good agreement with station observations. The modeling skill for aerosols, using ^{137}Cs as a proxy, was reduced, but no systematic bias was observed within the uncertainties related to the higher complexity of modeling the removal processes. For both xenon and cesium isotopes, emission source estimates derived by inverse modeling were used [15]. For ^{131}I , there was systematic model underestimation of station observations, but within the high uncertainty introduced by the emission source estimate used [16]. Since ^{131}I is removed from the atmosphere by radioactive decay rather than deposition processes and the test with ^{133}Xe indicated good agreement for the transport processes, the systematic underestimate of modeled ^{131}I was likely related to

underestimated ^{131}I sources in the model, which were based on literature data. The study confirmed the applicability of our global chemistry circulation model for simulating radionuclide transport from NPP accidents, as performed in the present study.

2.1. Emissions

All currently operational (189), under construction (16) and planned or proposed (36) nuclear reactors worldwide are included, based on the World Nuclear Association (WNA) reactor database (241 sites in total). Figure 1 shows the geographical distribution of potential emission locations. The distribution by country is listed in [4].

Figure 1. Geographical distribution of emission sites corresponding to nuclear power plants that are operational (red circles), under construction (green crossed circles) and planned or proposed (blue squares), adapted from [4]. Source: World Nuclear Association (WNA) Reactor Database.



Due to the limited availability of computational resources, the latter being tremendous for a high-resolution global model, it was not feasible to simulate varying emission height profiles. The graphite core material that burned in an open fire in Chernobyl, Ukraine, is meanwhile deprecated technology. Accidents that are lower on the INES scale and much more frequent in occurrence are more likely associated with radioactive leaks at the surface level. To account for different likelihoods, we use a point source at 1,000 hPa, equivalent to a mean height of approximately 100 m above the surface.

2.1.1. Eastern Mediterranean and Middle East

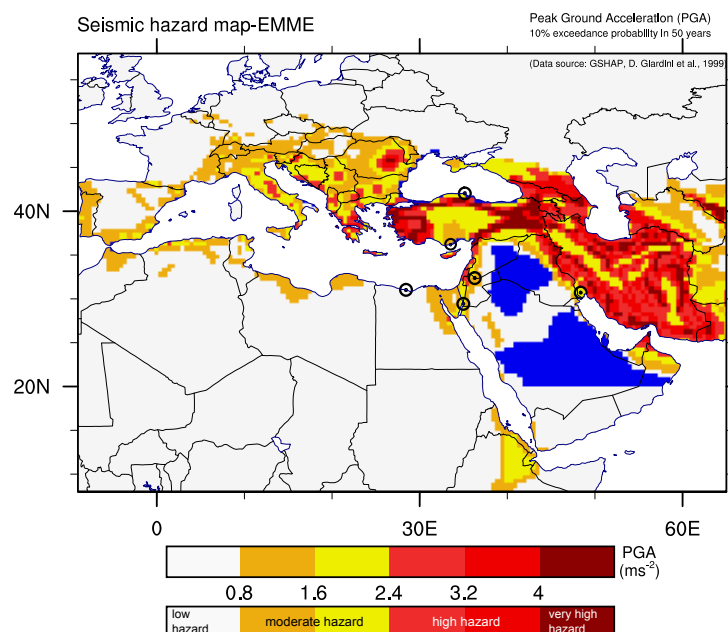
The Eastern Mediterranean and the Middle East (EMME) are made up of two dozen countries with approximately 400 million inhabitants. A number of countries in the region have planned or proposed the construction and operation of nuclear power plants.

A list of sites that are planned or proposed as locations for nuclear power plants in the EMME region is given in Table 1 and can be seen in Figure 2. We have selected the countries in the EMME region for a high resolution risk evaluation test case due to the high regional seismic risk, a potential cause of accidents. The Global Seismic Hazard Assessment Program (GSHAP) [17] and, in particular, the compilation of the GSHAP regional seismic hazard for Europe, Africa and the Middle East [18] report enhanced seismic hazard along the African Rift zone and across the Alpine-Himalayan belt, where there is a general eastward increase in hazard, with peak levels in Greece, Turkey, Caucasus and Iran (Figure 2). Figure 2 also illustrates that 5 out of 6 NNPs in the EMME are planned in moderate seismic hazard locations, while 3 NPPs will be situated within a few dozen kilometers from high hazard regions.

Table 1. Countries in the Eastern Mediterranean and the Middle East (EMME) region, where nuclear power plants are under construction or being planned, according to the World Nuclear Association (WNA) database.

Country	Code	Site	Latitude (°)	Longitude (°)
Egypt	EG	El Dabaa	31.03	28.44
Iran	IR	Darkhovin	30.71	48.38
Jordan	JO	Aqaba	29.43	34.98
Jordan	JO	Al Mafraq	32.37	36.28
Turkey	TR	Akkuyu	36.14	33.54
Turkey	TR	Sinop	42.03	35.15

Figure 2. Geographical distribution of emission sites corresponding to nuclear power plants that are under construction or planned in the EMME region (black circles, source: WNA Reactor Database), superposed on a map of the regional seismic hazard to peak ground acceleration (50-year 10% exceedance probability), adapted from the Global Seismic Hazard Assessment Program (GSHAP) [17,18]. Blue regions indicate no data available.



2.2. Atmospheric Dispersion

The iodine and cesium radionuclides are emitted as gases and partition into ambient aerosol particles at the relatively low temperatures in the ambient atmosphere, depending on the volatility of the gases.

The low solubility of iodine is based on publicly-available reported measurements [19]. Thus, ^{131}I (half life: 8.025 ± 0.002 days) is treated as being purely in the gas phase in our model and is largely removed from the atmosphere via radioactive decay. This allows for the reduction of computational complexity and for the direct comparison of gaseous and aerosol components of radioisotopes and is a valid approximation, as the atmospheric gaseous to particulate fraction is estimated to be close to a factor of four by a number of relevant measurements: the RadNet station network, operated by the U.S. Environmental Protection Agency (EPA), finds 81% of the ambient ^{131}I in the gas phase and 19% in the particulate phase [1]. The informal network of European national authorities, known as the Ring of Five (Ro5), comprising more than 150 high volume sampling systems, measures an average ratio of gaseous/total ^{131}I of $77.2\% \pm 13.6\%$ [20]. Both of these values are in agreement with the average values reported for the Chernobyl accident [21] and for the Fukushima site during the period spanning from March 22 to April 4, 2011 (ratio of $71\% \pm 11\%$) [22]. Therefore, a factor of 4 gaseous to particle phase partitioning would be appropriate. Dry deposition and particle sedimentation remove only up to 5%–10% of the emissions. We are not taking into account particle resuspension, expected to affect a negligible fraction of the deposited and sedimented quantities considered here.

The low-volatile ^{137}Cs (half-life: 30.17 ± 0.03 years) is modeled as a water-soluble aerosol with a standard lognormal distribution of mean radius $0.25 \mu\text{m}$, Henry's coefficient of $1.0 \text{ mol L}^{-1} \text{ atm}^{-1}$ and a density of $1,000.0 \text{ kg m}^{-3}$. The mean radius used is representative of the distribution of atmospheric aerosol in the accumulation mode size and most influenced by washout and rainout effects. It is consistent with the measurements of radioactivity after Chernobyl [23]. ^{137}Cs is removed from the atmosphere predominantly through small-scale convective and large-scale stratiform precipitation (90%–95% combined) and through dry deposition and sedimentation (5%–10% combined). The removal of accumulation mode particles by wet and, to a much lesser extent, by dry deposition is not sensitive to the assumed mean radius, as the scavenging efficiency of the accumulation mode particles in our model is not size dependent. The radioactive decay of ^{137}Cs is not taken into account in the simulation due to the long half-life of ^{137}Cs compared to the atmospheric residence time [24].

3. Results and Discussion

Our study uses a constant emission rate for the simulations, so that we obtain representative concentrations for all meteorological conditions, over which we subsequently average to derive the integral risks. Our results do not realistically represent the impact of any individual NPP accident under specific meteorological conditions, which would require a deterministic approach to represent an actual accident, but rather, aim to estimate the risk associated with all possible atmospheric states.

It is noted that, for the purposes of our study, the overall concentration and deposition magnitudes are renormalized, so that in each case, the highest risk corresponds to unity (arbitrary scale), *i.e.*, the relative geographical risk and equivalent dose are displayed. This allows for the scaling of the results to any accident severity level (defined by emission quantity) and also provides results for the subsequent

application of morbidity and mortality estimation models by other research groups that could provide such expertise.

3.1. Global Risk

The global mean (for the period 2010–2030) gaseous ^{131}I concentration relative risk from operating, under construction and planned nuclear power plants is shown in Figure 3. Presented are the mean global concentrations for the model surface layer (centered at around 30 m above the Earth's surface). The Southern Hemisphere concentration risk is found to be much lower, attributed to the low number of NPPs and the relatively short tracer half-life in combination with the relatively slow interhemispheric exchange in the atmosphere (characteristic time scale: about one year).

Figure 3. Combined total (operating, under construction, planned or proposed) relative risk by ^{131}I and equivalent daily effective dose to the public from inhalation over the 2010–2030 period; after [4].

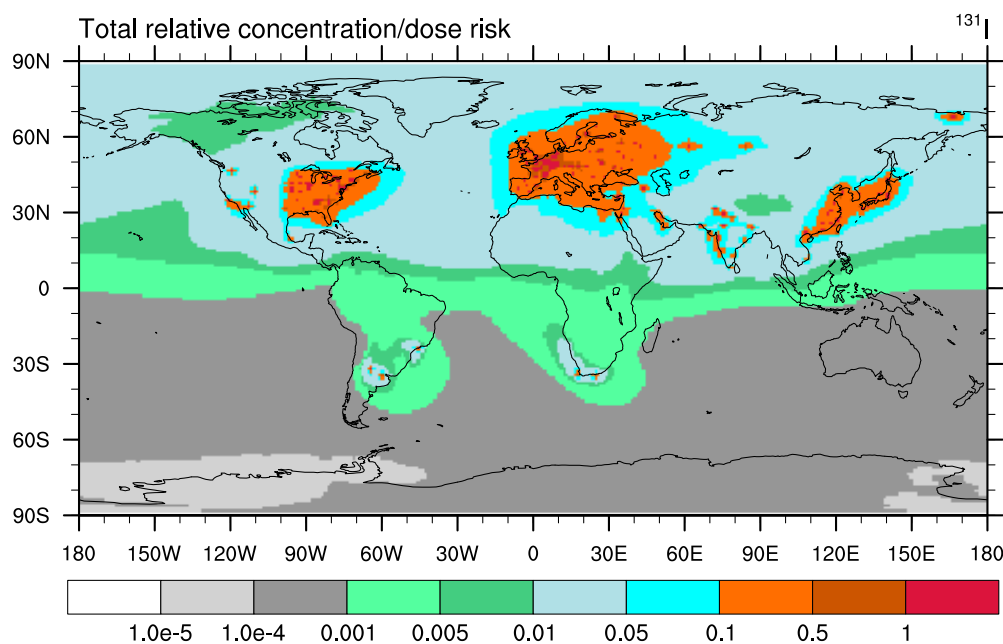
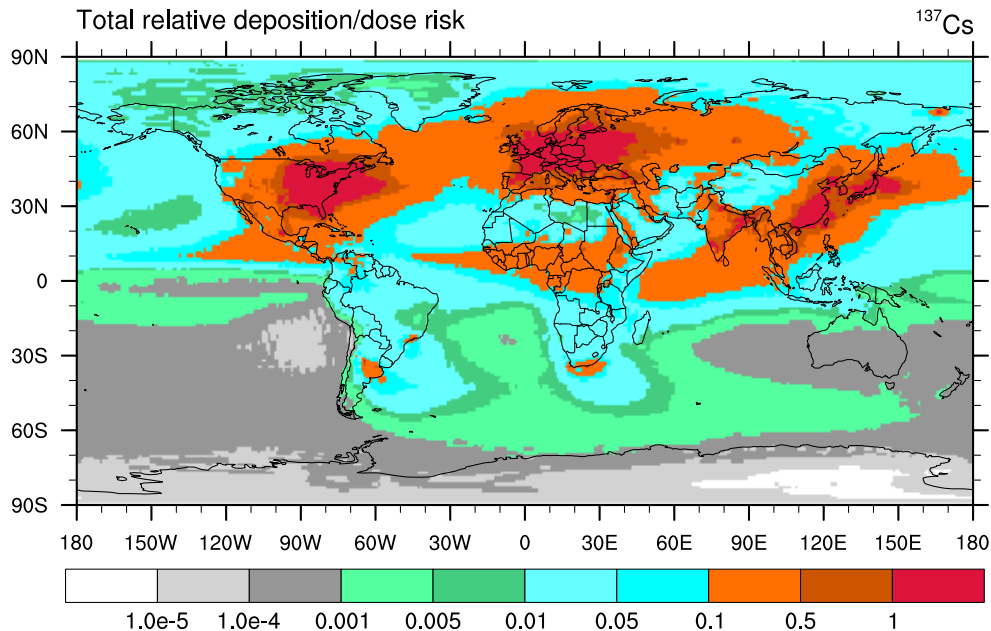


Figure 4 shows the global total cumulative surface deposition of ^{137}Cs over the period 2010–2030. The peak levels of deposition and, hence, the highest risk of ground contamination and population doses are expected in the eastern and central United States, across the European continent and along the Pacific coast of China, where most of the NPPs are located. The high rates of precipitation in the moist tropics result in enhanced risk due to wet deposition processes. This explains the relatively high risks in central Africa and southeastern Asia, where no or few NPPs are located, being downwind of NPPs in the EMME and western Asia, respectively.

Figure 4. Combined total (operating, under construction, planned or proposed) relative risk by cumulative dry and wet deposition and sedimentation of ^{137}Cs at the surface from nuclear accidents and equivalent effective dose risk to the population from exposure-related ground contamination over the 2010–2030 period; after [4].



It should be emphasized that aerosol removal processes occurring at the sub-grid scale are not explicitly simulated, but are parameterized [11,12] and, therefore, less well-resolved than processes affected by atmospheric dynamics and transport at the scale of the model resolution.

Changes in the global nuclear energy sector are decided at the national level. Results for the relative concentration, deposition and equivalent human population dose at the individual country level are provided in [4] and the accompanying supplement. The geographical distribution of the human population is also taken into account by defining a risk index as the relative risk in our model (from concentration and deposition separately) times the density of the population that can potentially be exposed for each country.

3.2. EMME Region

The regional mean gaseous ^{131}I concentration from proposed and planned nuclear power plants in the relatively high seismic hazard EMME region is shown in Figure 5. To estimate the concentration risk, we present the surface layer concentration based on the continuous uniform release of radionuclides from each NPP. For all plants, the concentrations in more remote locations are much lower, because of the relatively short half-life of ^{131}I (~ 8 days), which does not allow it to be transported over long distances and mix globally. Next, we briefly address the planning of NPPs in individual countries within the EMME region.

Jordan imports most of its energy and seeks greater energy security, as well as lower electricity prices. It is aiming to have a 1,000 MWe (Megawatt electric) nuclear power unit in operation by 2021 and a second one by 2025.

Figure 5. Individual and combined bottom relative surface level gaseous ^{131}I concentration and human population dose risk from potential nuclear power plant (NPP) accidents in the EMME region stations.

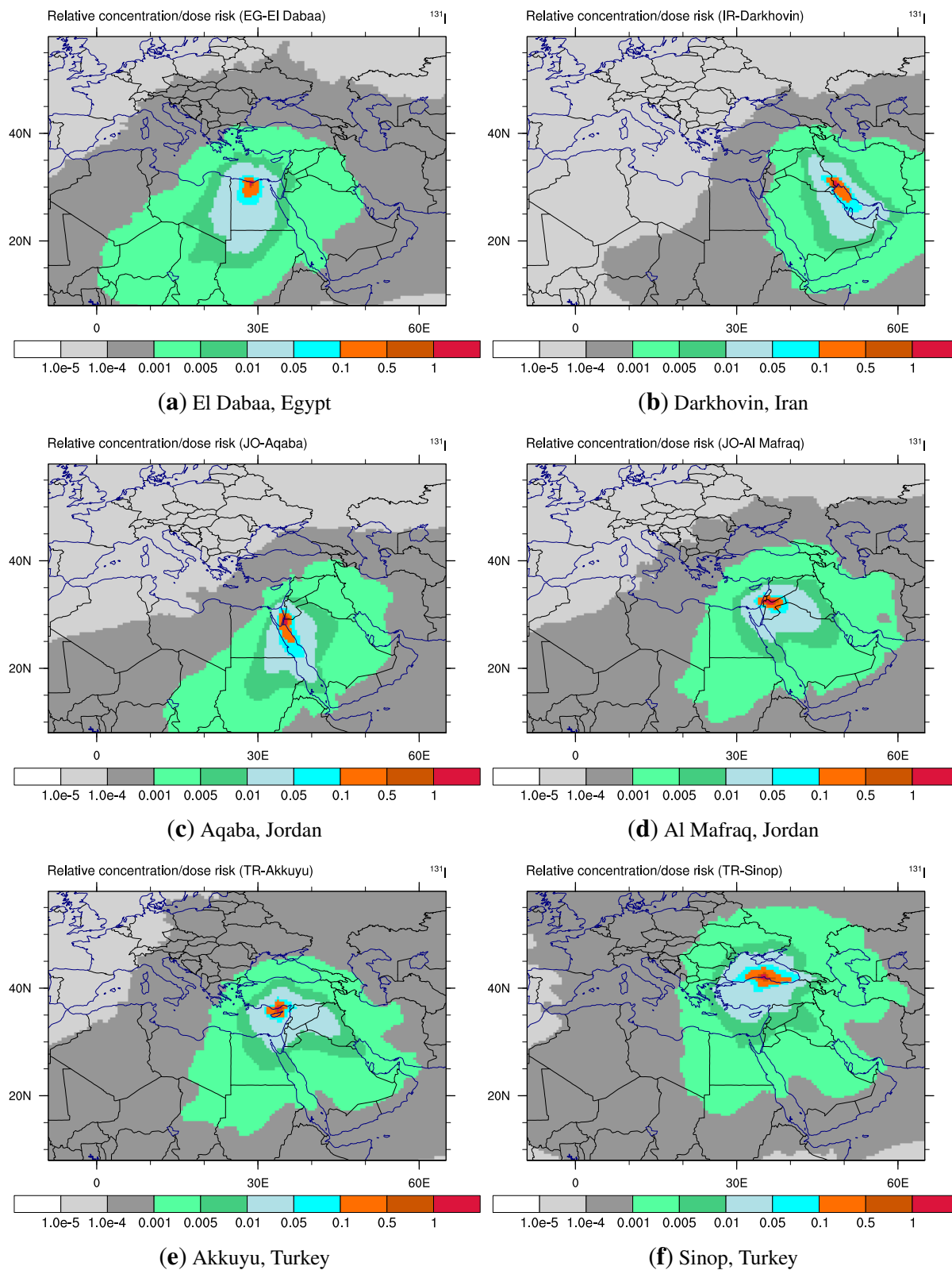
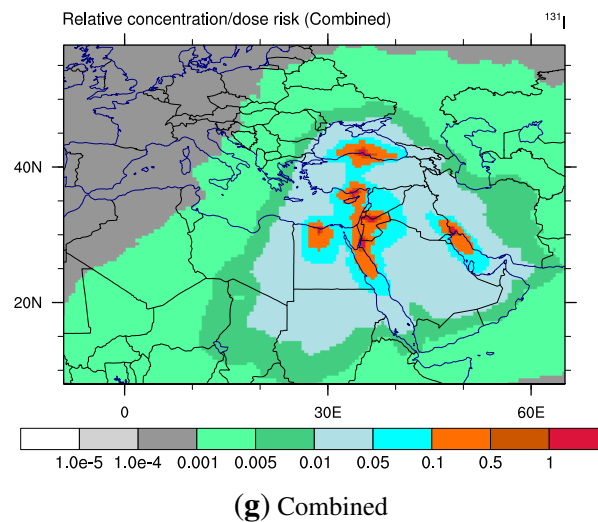


Figure 5. Cont.



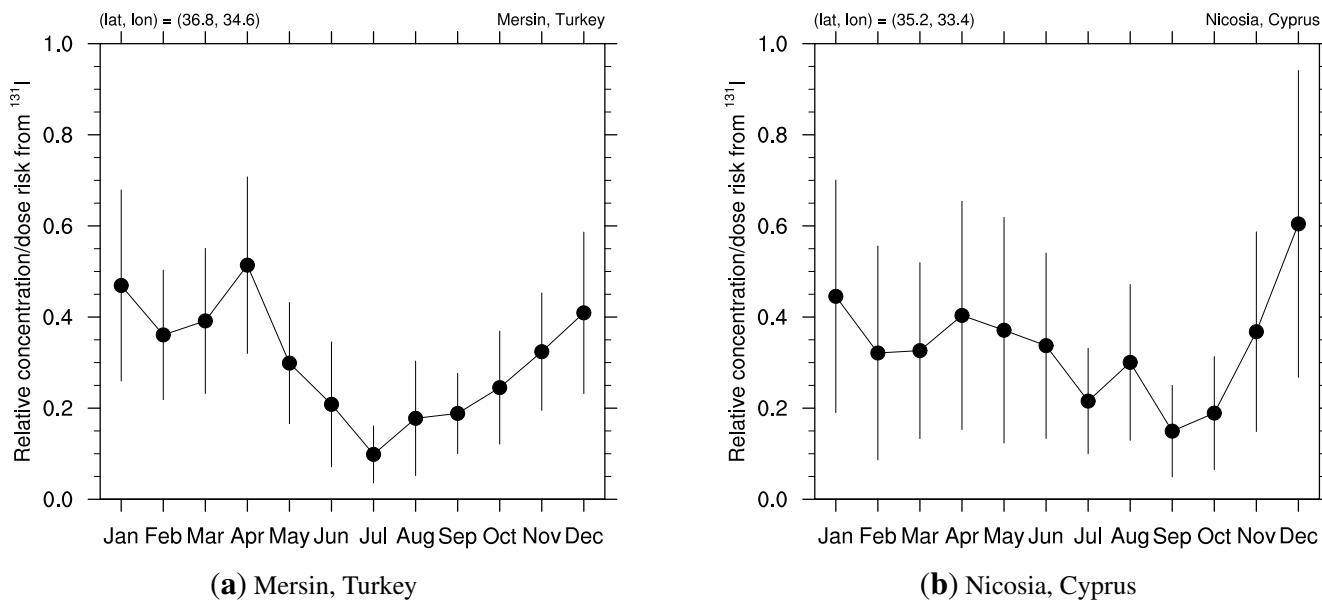
Turkey has been developing plans for establishing nuclear power generation for many decades. Meanwhile, nuclear power is a key aspect of the country's economic growth objectives. Recent developments have been supported by Russia, taking a leading role in financing and building 4,800 MWe of capacity. Applications are in progress for construction and operating licenses for the first plant at Akkuyu. A Franco-Japanese consortium is expected to build a second nuclear plant in Sinop.

Iran is currently operating a large nuclear power reactor, after many years of construction, and a second one is planned, though not formally according to the WNA database. Iran has not suspended its enrichment-related activities, nor its work on heavy water-related projects, as required by the UN Security Council.

Egypt has advanced plans, but commitments are pending. In April, 2013, Egypt approached Russia to renew the nuclear cooperation agreement, aiming for the construction of a nuclear power plant at El Dabaa. In November, 2013, the Russian Foreign Minister announced that Russia is prepared to finance and help construct an Egyptian nuclear plant.

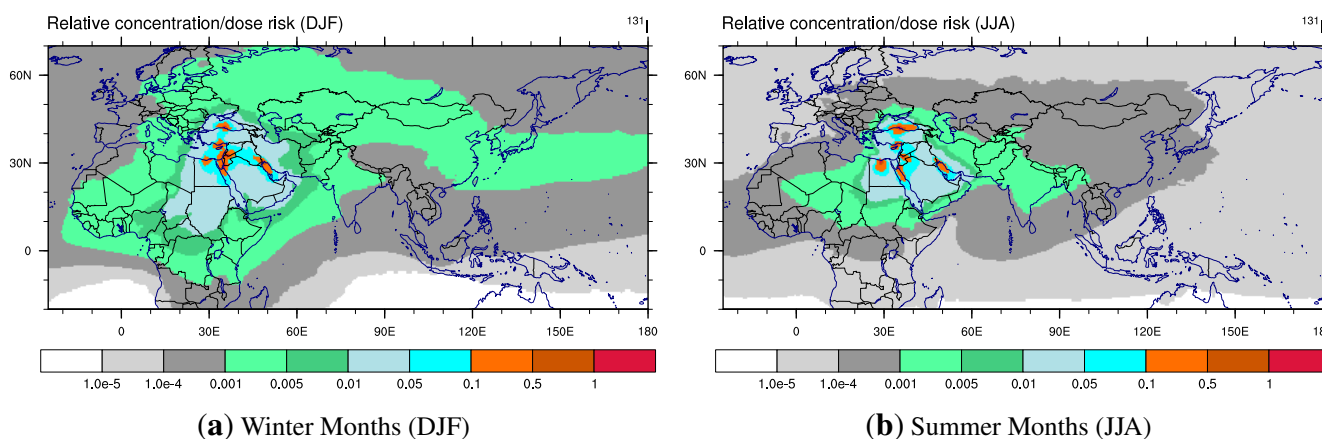
Figures 3 and 4 show that the relative risk in the Mediterranean region, due to the prevailing northerly and westerly winds, is relatively large due to atmospheric transport of contaminants from Europe. This meteorological regime will also affect radioactivity emissions from Akkuyu in southern Turkey, which will predominantly affect the island of Cyprus (Figure 5). The monthly mean relative ^{131}I surface concentration and associated dose risk from the Akkuyu NPP for the cities of Mersin, Turkey, and Nicosia, Cyprus, can be seen in Figure 6. Despite the relatively large uncertainties associated with the variable meteorological conditions at particular locations, Figure 6 illustrates that the risks are comparable in the two major cities closest to the NPP in neighboring countries. Unilateral decisions by countries to build NPPs do not do justice to the international consequences of potential reactor accidents. Figure 5 shows that the risks associated with the El Dabaa NPP (northern Egypt) are largest in Egypt and of Sinop (northern Turkey) in Turkey, while the other operational and planned NPPs in the EMME region are associated with significant trans-boundary risks.

Figure 6. Monthly mean relative ^{131}I surface concentration and associated dose risk from a potential accident at the Akkuyu NPP for the cities of Mersin, Turkey (a), and Nicosia, Cyprus (b).



The model-calculated risk from the climatological mean surface level concentration of radionuclides (Figure 7) exhibits strong seasonal variability.

Figure 7. Relative seasonal risk by ^{131}I (mean surface layer concentration) from potential NPP accidents and equivalent effective dose to the public from inhalation in the EMME region for the winter (a) and summer months (b).



Our model shows increased surface-level concentrations throughout the Northern Hemisphere during the boreal winter months (DJF) compared to the summer months (JJA). Not only the expected risk magnitude is higher, but the geographical extent of the high concentrations of transported radionuclides is more pronounced towards the north over parts of Europe and Russia and towards the east over Asia. Horizontal advection is more efficient in winter due to relatively stronger winds, and the concentrations are highest near the surface, because of the lower vertical development of the atmospheric planetary boundary layer. As a result, the surface level concentrations in the summer tend to be more localized in the emission region, whereas dilution by turbulent mixing and vertical transport by deep convective

clouds is more efficient. This is in line with our previous work examining the global combined total seasonal variation for all stations [4], where the aerosol radionuclide deposition was also assessed. The total mass of aerosol ^{137}Cs in the atmosphere was similarly found to be lower in winter and higher during summer, due to more efficient removal by wet deposition processes.

3.3. Uncertainty

To quantitatively assess the uncertainty of the risk estimates from the simulated temporal variability, we use the coefficient of variation (the local standard deviation σ over the mean μ) for individual NPPs in the EMME region and their combined total, shown in Figure 8. The equivalent uncertainty analysis for all NPPs globally can be found in [4].

The regional variability does not exceed 15% (typical values around 7%), with the highest values found in close proximity of the region of interest and further northeast in the Northern Hemisphere, as well as over the continent of Africa in the Southern Hemisphere, notably in the vicinity of Madagascar. This is understood as the effects of the trade winds, causing equatorward transport of radionuclides and convective overturning in the intertropical convergence zone to the south of the EMME region, followed by subsidence in the subtropical Southern Hemisphere. This effect is most pronounced for the Darkhovin NPP in Iran. Elsewhere, the coefficient of variation is well within 5%, signifying adequate coverage for our analysis sample size and appropriate representation of the temporal circulation variability effects, especially considering the associated uncertainties of the global representation of modeled processes.

Figure 8. Individual and combined bottom relative risk coefficient of variation (σ/μ) for NPPs in the EMME region.

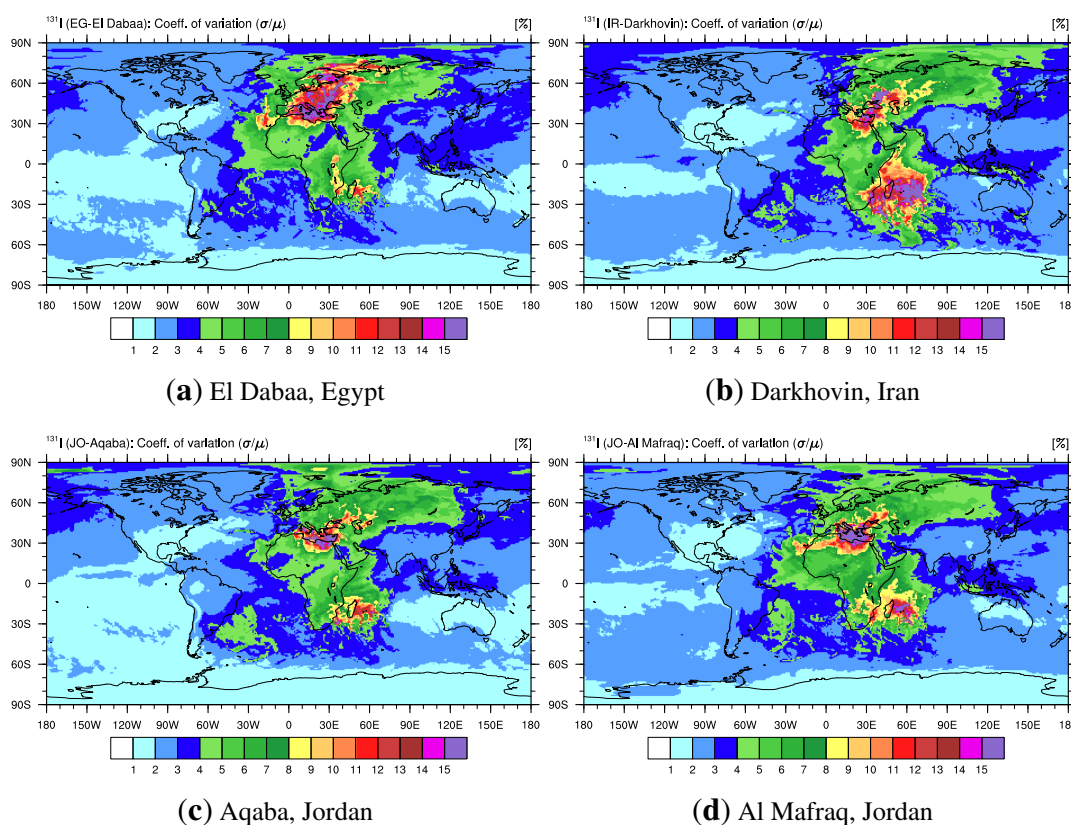
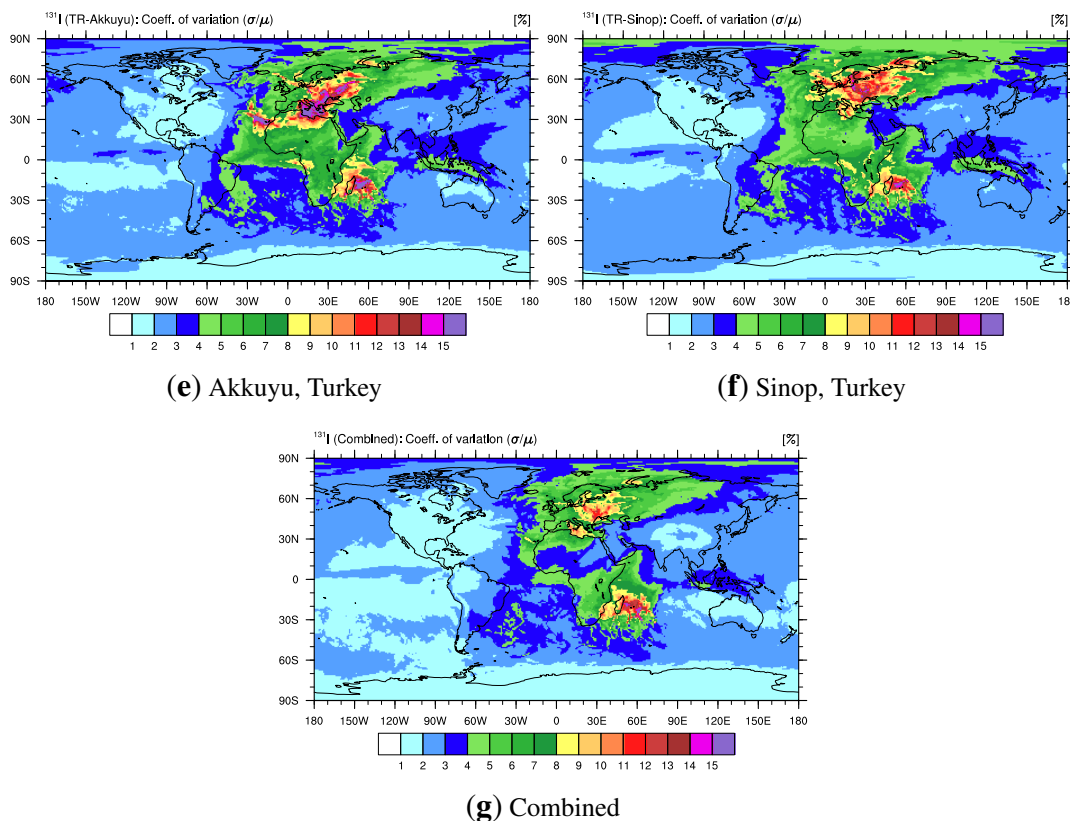


Figure 8. Cont.



4. Conclusions

The EMAC atmospheric chemistry-general circulation model was used to assess the global risks from the atmospheric dispersion of radioactivity from potential accidents at nuclear power plants (years 2010–2030, 11-km equivalent horizontal grid resolution). We also performed a particularly high model resolution case study encompassing NPPs that are under construction, planned or proposed to be operated in the EMME region (meteorology of the years 2003–2009, ~50-km equivalent resolution), a region with a relatively high seismic hazard. The model simulations were driven by boundary conditions from the AMIP II simulations for the recent past and the IPCC SRES A2 scenario for the future projections. This paper both complements and extends our previous study of the global risk from all nuclear power stations that are in operation, under construction and planned or proposed.

We have calculated the relative surface concentrations for the gaseous radionuclide ^{131}I and surface deposition for particulate ^{137}Cs , which correspond to equivalent risks for the human population to be exposed to radioactivity from hypothetical accidents at NPPs. Reporting the relative exposure allows scaling of the results to any individual NPP accident based on the real or estimated magnitude of radionuclide emissions, which can be used to project morbidity and mortality risks by using our findings as input to impact assessments for particular levels of radioactivity.

As can be expected, the areas in the vicinity of the individual NPPs in the EMME region are at the highest risk, while the medium- and long-range transport through the atmosphere does not exhibit uniform dispersion. Land masses to the south and east of the region show a significantly higher risk

expectation, in particular from the combination of all NPPs in the region. Our results illustrate that accidents at many of the operational or planned NPPs in the region could have significant trans-boundary consequences.

The risk estimate for all planned stations in the EMME region and their combined total risk exhibit strong seasonal variability, with increased surface level concentrations of gaseous radionuclides in the Northern Hemisphere during winter and a larger geographical extent towards the north and the east for the higher-risk affected areas. This is related to the relatively shallow boundary layer in winter that confines the emitted radioactivity to the lowest part of the atmosphere close to the surface.

The coefficient of variation, defined as the simulated local temporal standard deviation relative to the mean (σ/μ), was used as a measure of the uncertainty in the risk estimates for individual NPPs and the combined total for our study. For all cases, outside the vicinity of the NPPs, the regional variability does not exceed 15% (with typical values around 7%), signifying adequate temporal coverage by the simulation period and being climatically representative.

It is the view of the authors that it is imperative to assess the risks from the atmospheric dispersion of radioactivity from potential NPP accidents, particularly for regions with high seismic, as well as other natural and human activity-related hazards in order to facilitate preparedness and emergency response planning on national and international levels.

Acknowledgments

The research leading to these results has received funding from the European Research Council under the European Union's Seventh Framework Programme (FP7/2007–2013)/ERC Grant Agreement No. 226144. This work was supported by the Cy-Tera Project, which is co-funded by the European Regional Development Fund and the Republic of Cyprus through the Research Promotion Foundation. The Climate Data Operators (CDO) [25], netCDF operators (NCO) [26] and the National Center for Atmospheric Research (NCAR) Command Language (NCL) [27] were used for data processing and visualization.

Author Contributions

Theodoros Christoudias and Yiannis Proestos: Model Development, Data Analysis, Manuscript Writing; Jos Lelieveld: Manuscript Writing, Study Overview.

Abbreviations/Nomenclature

EMME	Eastern Mediterranean and Middle East
NPP	nuclear power plant
IAEA	International Atomic Energy Agency
INES	IAEA International Nuclear Event Scale
CTBTO	Comprehensive Nuclear-Test-Ban Treaty Organization
WNA	World Nuclear Association
GSHAP	Global Seismic Hazard Assessment Program
SRES	Special Report on Emission Scenarios

Conflicts of Interest

The authors declare no conflict of interest.

References

1. Ten Hoeve, J.E.; Jacobson, M.Z. Worldwide health effects of the Fukushima Daiichi nuclear accident. *Energy Environ. Sci.* **2012**, *5*, 8743–8757.
2. Arnold, D.; Gufler, K.; Kromp, W.; Kromp-Kolb, H.; Mraz, G.; Seibert, P.; Sholly, S.; Sutter, P.; Wenisch, A. flexRISK—Flexible tools for assessment of nuclear risk in Europe. In *Air Pollution Modeling and Its Application XXI*; Springer: Dordrecht, The Netherlands, 2012; pp. 737–740.
3. Lelieveld, J.; Kunkel, D.; Lawrence, M. Global risk of radioactive fallout after major nuclear reactor accidents. *Atmosp. Chem. Phys.* **2012**, *12*, 4245–4258.
4. Christoudias, T.; Proestos, Y.; Lelieveld, J. Global risk from the atmospheric dispersion of radionuclides by nuclear power plant accidents in the coming decades. *Atmosp. Chem. Phys.* **2014**, *14*, 4607–4616.
5. Jöckel, P.; Kerkweg, A.; Pozzer, A.; Sander, R.; Tost, H.; Riede, H.; Baumgaertner, A.; Gromov, S.; Kern, B. Development cycle 2 of the Modular Earth Submodel System (MESSy2). *Geosci. Model Dev.* **2010**, *3*, 717–752.
6. Roeckner, E.; Bäuml, G.; Bonaventura, L.; Brokopf, R.; Esch, M.; Giorgetta, M.; Hagemann, S.; Kirchner, I.; Kornbluh, L.; Manzini, E.; *et al.* *The Atmospheric General Circulation Model ECHAM5.PART I: Model Description*; Technical Report; Max Planck Institute for Meteorology: Hamburg, Germany, 2003.
7. Roeckner, E.; Brokopf, R.; Esch, M.; Giorgetta, M.; Hagemann, S.; Kornbluh, L.; Manzini, E.; Schlese, U.; Schulzweida, U. *The Atmospheric General Circulation Model ECHAM5. PART II: Sensitivity of Simulated Climate to Horizontal and Vertical Resolution*; Technical Report MPI-Report 354; Max Planck Institute for Meteorology: Hamburg, Germany, 2004.
8. Taylor, K.E.; Williamson, D.; Zwiers, F. *The Sea Surface Temperature and Sea-Ice Concentration Boundary Conditions for AMIP II Simulations*; Program for Climate Model Diagnosis and Intercomparison, Lawrence Livermore National Laboratory; University of California: Livermore, CA, USA, 2000.
9. Nakicenovic, N.; Alcamo, J.; Davis, G.; de Vries, B.; Fenhann, J.; Gaffin, S.; Gregory, K.; Grübler, A.; Jung, T.Y.; Kram, T.; *et al.* *Special Report on Emissions Scenarios, Working Group III*; Intergovernmental Panel on Climate Change (IPCC): Geneva, Switzerland, 2000.
10. Kerkweg, A.; Sander, R.; Tost, H.; Jöckel, P. Technical Note: Implementation of prescribed (OFFLEM), calculated (ONLEM), and pseudo-emissions (TNUDGE) of chemical species in the Modular Earth Submodel System (MESSy). *Atmos. Chem. Phys.* **2006**, *6*, 3603–3609.
11. Tost, H.; Jöckel, P.; Kerkweg, A.; Sander, R.; Lelieveld, J. Technical Note: A new comprehensive SCAVenging submodel for global atmospheric chemistry modelling. *Atmos. Chem. Phys.* **2006**, *6*, 565–574.

12. Tost, H.; Jöckel, P.; Kerkweg, A.; Pozzer, A.; Sander, R.; Lelieveld, J. Global cloud and precipitation chemistry and wet deposition: Tropospheric model simulations with ECHAM5/MESSEy1. *Atmosp. Chem. Phys.* **2007**, *7*, 2733–2757.
13. Ritchie, H.; Temperton, C.; Simmons, A.; Hortal, M.; Davies, T.; Dent, D.; Hamrud, M. Implementation of the semi-Lagrangian method in a high-resolution version of the ECMWF forecast model. *Mon. Weather Rev.* **1995**, *123*, 489–514.
14. Christoudias, T.; Lelieveld, J. Modelling the global atmospheric transport and deposition of radionuclides from the Fukushima Dai-ichi nuclear accident. *Atmos. Chem. Phys.* **2013**, *13*, 1425–1438.
15. Stohl, A.; Seibert, P.; Wotawa, G.; Arnold, D.; Burkhardt, J.; Eckhardt, S.; Tapia, C.; Vargas, A.; Yasunari, T. Xenon-133 and caesium-137 releases into the atmosphere from the Fukushima Dai-ichi nuclear power plant: Determination of the source term, atmospheric dispersion, and deposition. *Atmosp. Chem. Phys.* **2012**, *12*, 2313–2343.
16. Chino, M.; Nakayama, H.; Nagai, H.; Terada, H.; Katata, G.; Yamazawa, H. Preliminary estimation of release amounts of ¹³¹I and ¹³⁷Cs accidentally discharged from the Fukushima Daiichi nuclear power plant into the atmosphere. *J. Nucl. Sci. Technol.* **2011**, *48*, 1129–1134.
17. Giardini, D.; Grünthal, G.; Shedlock, K.M.; Zhang, P. The GSHAP global seismic hazard map. *Ann. Geophys.* **1999**, *42*, 1225–1230.
18. Grünthal, G.; Bosse, C.; Sellami, S.; Mayer-Rosa, D.; Giardini, D. Compilation of the GSHAP regional seismic hazard for Europe, Africa and the Middle East. *Annal. Geofis.* **1999**, *42*, 1215–1223.
19. Weast, R.C.; Astle, M.J.; Beyer, W.H. *CRC Handbook of Chemistry and Physics*; CRC Press: Boca Raton, FL, USA, 1988; Volume 69.
20. Masson, O.; Baeza, A.; Bieringer, J.; Brudecki, K.; Bucci, S.; Cappai, M.; Carvalho, F.; Connan, O.; Cosma, C.; Dalheimer, A.; *et al.* Tracking of airborne radionuclides from the damaged Fukushima Dai-ichi nuclear reactors by European networks. *Environ. Sci. Technol.* **2011**, *45*, 7670–7677.
21. Hilton, J.; Cambray, R.; Green, N. Chemical fractionation of radioactive caesium in airborne particles containing bomb fallout, Chernobyl fallout and atmospheric material from the Sellafield site. *J. Environ. Radioact.* **1991**, *15*, 103–111.
22. Stoehlker, U.; Nikkinen, M.; Gheddou, A. Detection of radionuclides emitted during the Fukushima nuclear accident with the CTBT radionuclide network. In Proceedings of the Monitoring Research Review 2011: Ground-Based Nuclear Explosion Monitoring Technologies, Tucson, AZ, USA, 13–15 September 2011; pp. 715–724.
23. International Atomic Energy Agency (IAEA). *Environmental Consequences of the Chernobyl Accident and Their Remediation: Twenty Years of Experience*; IAEA: Vienna, Austria, 2006.
24. Kristiansen, N.; Stohl, A.; Wotawa, G. Atmospheric removal times of the aerosol-bound radionuclides ¹³⁷Cs and ¹³¹I measured after the Fukushima Dai-ichi nuclear accident—A constraint for air quality and climate models. *Atmosp. Chem. Phys.* **2012**, *12*, 10759–10769.
25. Schulzweida, U. *CDO User's Guide, Version 1.6.0*; MPI for Meteorology: Hamburg, Germany, 2013.

26. Zender, C.S. *NCO User's Guide, Version 4.3.5*; University of California: Irvine, CA, USA, 2013.
27. UCAR/NCAR/CISL/VETS. *The NCAR Command Language (Version 6.0.0) Software*. National Center for Atmospheric Research: Boulder, CO, USA, 2012.

© 2014 by the authors; licensee MDPI, Basel, Switzerland. This article is an open access article distributed under the terms and conditions of the Creative Commons Attribution license (<http://creativecommons.org/licenses/by/4.0/>).